De novo genome assemblies from two Indigenous Americans from Arizona identify new polymorphisms in non-reference sequences

Çiğdem Köroğlu[1], Peng Chen[1], Michael Traurig[1], Serdar Altok[2], Clifton Bogardus[1], Leslie J Baier[1]

[1]Diabetes Molecular Genetics Section, Phoenix Epidemiology and Clinical Research Branch, National Institute of Diabetes and Digestive and Kidney Diseases, National Institutes of Health, Phoenix, AZ, USA

[2]Independent Researcher, Phoenix, AZ, USA

Corresponding Author:

Leslie J. Baier, PhD

445 North 5th Street, Phoenix, AZ 85004, USA

Phone: +1 602 440 6589 (office); Fax: +1 602 253 4140

E-mail: lbaier@phx.niddk.nih.gov

Short title: Analysis of non-reference sequences in Indigenous American genomes

Word count: 4,150 (excluding abstract, author summary, and references)

ABSTRACT

There is a collective push to diversify human genetic studies by including underrepresented populations. However, analyzing DNA sequence reads involves the initial step of aligning the reads to the GRCh38/hg38 reference genome which is inadequate for non-European ancestries. To help address this issue, we created a modified hg38 reference map using *de novo* sequence assemblies from Indigenous Americans living in Arizona (IAZ). Using HiFi SMRT long-read sequencing technology, we generated *de novo* genome assemblies for one female and one male IAZ individual. Each assembly included ~17 Mb of DNA sequence not present (non-reference sequence; NRS) in hg38, which consists mostly of repeat elements. Forty NRSs totaling 240 kb were uniquely anchored to the hg38 primary assembly generating a modified hg38-NRS reference genome. DNA sequence alignment and variant calling were then conducted with WGS sequencing data from 387 IAZ cohorts using both the hg38 and modified hg38-NRS reference maps. Variant calling with the hg38-NRS map identified ~50,000 single nucleotide variants present in at least 5% of the WGS samples which were not detected with the hg38 reference map. We also directly assessed the NRSs positioned within genes. Seventeen NRSs anchored to regions including an identical 187 bp NRS found in both de novo assemblies. The NRS is located in *HCN2* 79 bp downstream of exon 3 and contains several putative transcriptional regulatory elements. Genotyping of the *HCN2*-NRS revealed that the insertion is enriched in IAZ (MAF = 0.45) compared to Caucasians (MAF = 0.15) and African Americans (MAF = 0.03). This study shows that inclusion of population-specific NRSs can dramatically change the variant profile in an under-represented ethnic groups and thereby lead to the discovery of previously missed common variations.

AUTHOR SUMMARY

GRCh38/hg38 reference genome has been the standard reference for large-scale human genetics studies. However, it does not adequately represent sequences of non-European ancestry. In this study, using long-read sequencing technology, we constructed *de novo* sequence assemblies from two Indigenous Americans from Arizona. We then compared the *de novo* assemblies to the hg38 reference genome to identify non-reference sequences (NRSs). We integrated these NRSs into our whole-genome sequencing (WGS) variant calling pipeline to improve read alignment and variant detection. We also directly assessed the NRSs positioned within genes. Inclusion of population-specific NRSs dramatically changed the variant profile of our study group with under-represented ethnicity, revealing common variation not detected by our previous population-level WGS and genotyping studies.

INTRODUCTION

The lack of diversity in human genetic studies is of growing concern, particularly as personalized medicine is becoming a reality. The majority of genomics data, approximately 80 percent, predominantly represents individuals of European ancestry, highlighting a significant underrepresentation of other populations [1]. This lack of diversity has had adverse consequences in genetic testing and variant interpretation, particularly for patients of African and Asian ancestry [2,3]. Recent large-scale genome studies, such as the All of Us initiative [4], the Human Heredity and Health in Africa (H3Africa) project [5], and the GenomeAsia100K project [6], have made significant efforts to address this disparity by actively increasing the representation of diverse populations. However, aside from the challenges associated with sample collection for sequencing, these endeavors face two main limitations when generating genomic data for underrepresented

70 populations. One limitation is due to short-read sequencing being the main method in large
71 population studies. While short-reads offers valuable insights through comparisons of allele
72 frequencies and functional annotations, they struggle to capture rare variants and accurately
73 characterize structural variants in isolated populations [7-9]. This restricts the comprehensive
74 understanding of genetic diversity and hampers the identification of variants associated with
75 diseases. The second limitation stems from the reliance on a human genome reference during DNA
76 sequence read analysis. The current reference map, the GRCh38/hg38 reference genome, primarily
77 comprises sequences derived from a single DNA donor of African-European origin, accounting
78 for approximately 70% of the primary assembly sequences [10]. Consequently, the current
79 reference map still exhibits limitations in adequately representing the genetic diversity found
80 within diverse populations. It is important to recognize that individuals may carry unique
81 sequences that are not represented in the reference map, thereby harboring genomic regions with
82 potential disease associations and other phenotypic relevance. Therefore, it has been imperative
83 for the genomic research in isolated populations to move beyond the traditional short-read
84 sequencing and linear reference genome paradigm.
85 Long-read sequencing technologies have boosted our power in resolving complex regions of the
86 genome, detecting structural variants, and assembling complete chromosomes [11-13]. In the
87 recent years, these technologies have advanced in accuracy and yield, enabling variant detection
88 at a large scale, with recent studies showcasing their potential in population-scale analyses [13,14].
89 Significant steps have also been taken to address the issue of the low ancestral diversity in the
90 human genome reference. The Human Pangenome Reference Consortium has been working on
91 constructing a reference that encompasses diverse genomes, and they have published the first draft
92 of the pangenome, consisting of 47 genome assemblies from a diverse cohort [15]. However, there

93 are still challenges to overcome in growing and refining this reference, both in sampling and in
94 computational analysis. The current sampling efforts do not include Indigenous American or
95 Aboriginal peoples (https://humanpangenome.org/samples/). Indigenous American people are
96 genetically distinct compared to other populations in the United States, with a significant variation
97 within the group itself [16]. Principal component analysis from a previous study including three
98 ancestral populations from the 1000 Genomes database (European, East Asian, and African
99 ancestries) and our Indigenous American population from Arizona (IAZ) showed a distinct cluster
100 for IAZ on the principal component space [17]. Therefore, exploratory genomics studies using
101 novel methods are warrented in indigenous populations to uncover previously unrecognized
102 genetic variations and capture novel disease associations.
103 In this study, we aimed to improve identification of genetic variations that have not been previously
104 studied among IAZ population. We utilized *de novo* genome assemblies to identify non-reference
105 segments (NRSs) in this cohort. These NRSs represent novel genomic segments not present in the
106 existing reference map. By analyzing these segments, both directly and by incorporating them into
107 our whole-genome sequencing (WGS) variant calling pipeline, we sought to uncover previously
108 unrecognized polymorphisms which can be assessed for a potential role in metabolic disease
109 enriched in this underrepresented ethnic group.
110

111 **RESULTS**

112 ***De novo* IAZ genome assemblies**

113 DNA samples from one female (sample 1) and one male (Sample 2) Indigenous American from
114 Arizona (IAZ) were sequenced using the PacBio HiFi SMRT sequencing platform. Summary
115 reports for the raw PacBio sequencing data are shown in S1 Table. For both samples, the SMRT

116 sequencing reactions produced approximately 64 Gb of high-fidelity subreads (>Q20) with a mean
117 length of ~12 kb, which were used to generate the *de novo* genome assemblies. Primary contigs
118 with high contiguity were generated using HiFiasm assembler (Table 1). Assembly 1 (female
119 IAZ) and assembly 2 (male IAZ) yielded a total genome length of 3.05 and 3.07 Gb, respectively,
120 indicating high assembly quality regarding genome completeness when compared to the 2.96 Gb
121 GRCh38/hg38 reference genome excluding gaps. Subsequent rounds of MUMmer alignment
122 identified 19 Mb and 17 Mb of DNA sequence for assembly 1 and assembly 2, respectively, that
123 could not be aligned to the hg38 reference genome. These non-reference sequences (NRSs) have
124 a minimum length of 100 bps and a hg38 sequence identity < 80%.

125
126 **Table 1. Summary statistics for the IAZ *de novo* assemblies.**

Contiguity metric	Assembly 1	Assembly 2
N50	48.04 Mb	36.34 Mb
NG50	41.32 Mb	32.19 Mb
Area under the N curve	46.30 Mb	39.89 Mb

127 Assembly 1, female IAZ individual. Assembly 2, male IAZ individual. N50 is the length
128 of the shortest assembled contig at 50% of the total assembly length. NG50 is the length
129 of the shortest assembled contig at 50% of the total genome length. For NG50 and area
130 under the N curve, 3.3 Gb of genome size is assumed.
131

132 **NRS size distribution for the IAZ *de novo* assemblies**

133 The two IAZ *de novo* assemblies had similar numbers of NRSs and size distribution patterns with
134 a total length of 19.3 Mb for assembly 1 (n = 2,177 NRSs) and 16.34 Mb for assembly 2 (n = 1908
135 NRSs) (Fig 1A-F). For both assemblies, most of the NRSs are 10 kb and shorter but only accounted
136 for 14.4% and 13.4% of the total lengths for assembly 1 and assembly 2 respectively (Fig 1A and
137 D). There were 130 NRSs for both assemblies with sizes greater than 10 kb–100 kb with medium
138 sizes of 20.5 kb for assembly 1 and 22.7 kb for assembly 2 (Fig 1B and E). 93 NRSs are larger
139 than 100 kb (assembly 1, n = 50; assembly 2 n = 43), including 3 outlier NRSs larger than 500 kb
140 (Fig 1C and F).

141

142 **Identification of repeat and transposable elements**

143 Screening the NRSs for repeat and transposable elements using RepeatMasker revealed that
144 approximately 95% of the NRSs in both assemblies primarily consisted of satellites, simple
145 repeats, and a small fraction of LINE and SINE transposable elements (S1 Fig). The three largest
146 NRSs with lengths of 637 kb, 1.88 Mb (assembly 1), and 1.47 Mb (assembly 2) were individually
147 analyzed for their repeat content. They consisted almost entirely of satellites and simple repeats
148 (ranging from 99.7% to 99.9%) rendering their alignment to chromosomes challenging.

149

150 **Mapping the NRSs to the GRCh38/hg38 reference genome**

151 NRSs totaling 241 kb could be placed into 40 distinct locations within the primary scaffold of
152 GRCh38/hg38. Only 4 of the NRSs totaling 7.6 kb were placed into centromeric regions
153 suggesting that there was no enrichment of centromeric DNA which is in contrast to long-read
154 sequencing projects involving other populations [18, 19]. However, when the alignments for all of
155 the NRSs with at least one anchored flanking site were analyzed, the percentage of NRSs aligning
156 to centromeric or telomeric regions was ~30%. The 233.4 kb non-centromeric NRSs includes a
157 large 215 kb insertion aligning to chrY and ~18.4 kb of NRS anchoring to 13 autosomal
158 chromosomes, chrX, and 2 pseudoautosomal regions on chrY. Among the 36 non-centromeric
159 NRSs, 17 are located within intronic regions of 13 protein coding and 4 non-protein-coding genes.
160 Three NRSs were present in both assemblies and only 1, *HCN2*-NRS, was identical in size and
161 therefore was selected for further characterization (Table 2). The *HCN2*-NRS in not present in the
162 reference genomes, including the T2T-CHM13 map, suggesting that the *HCN2*-NRS may not exist
163 in the DNA samples used for reference genome construction. *HCN2*-NRS is located 79 bp
164 downstream of exon 3 and replaces 228 bp of the reference sequence including a small portion of

165 a predicted cis-regulatory element (CRE). Individuals who carry the 187 bp HCN2-NRS also have
166 an adjacent 100 bp deletion (S2 Fig). The *HCN2*-NRS matches (100% identity) with 187 bps
167 downstream of exon 4 spanning a putative CRE containing various transcription factor binding
168 sites suggesting that *HCN2*-NRS may have functional importance (Fig 2, S2 Fig).

Table 2. Non-reference sequences anchoring within genes.

Gene	Insertion region[a]	NRS size (bps)	Both assemblies
LINC02270	Chr4:12237666–12237666	139	No
F11-AS1	Chr4:186435038–186435150	4714	No
BTNL9	Chr5:181046016–181046016	386	No
DYNC2I1	Chr7:158915724–158915724	679	No
MROH5	Chr8:141492602–141492602	1722	No
GTPBP4	Chr10:1011004–1011004	341	No
ART1	Chr11:3653879–3653937	877	Yes[b]
PDGFD	Chr11:104078565–104078565	579	No
LOC728715	Chr12:9404585–9404585	836	Yes[b]
GNPTAB	Chr12:101747637–101747644	658	No
MPG	Chr16:81854–81857	344	No
CACNA1H	Chr16:1186044–1186087	466	No
HCN2	Chr19:605301–605528	187	Yes
ADGRG2	ChrX:19074564–19074564	429	No
RGN	ChrX:47089179–47089179	1127	No
CRLF2	ChrY:1198256–1198271[c]	287	No
P2RY8	ChrY:1496850–1496850[c]	136	No

169 NRS, non-reference sequence. [a]Position based on GRCh38/hg38. Indicated intervals are replaced by NRSs.
170 [b]NRS sizes slightly different between the two assemblies. [c]Pseudoautosomal region.
171

172 **Population frequency and association analyses for *HCN2*-NRS**

173 To confirm the presence of the *HCN2*-NRS, the region encompassing the putative NRS was PCR
174 amplified and sequenced in the two IAZ individuals used for the *de novo* genome assembly along
175 with some of their family members. Of the 10 individuals sequenced, 1 was heterozygous and 9
176 were homozygous for *HCN2*-NRS suggesting that the NRS segment was common in the IAZ
177 population. To determine the frequency of *HCN2*-NRS in IAZ, ~3,400 IAZ individuals were
178 genotyped using a custom designed TaqMan probe that detects the presence of the NRS. The
179 *HCN2*-NRS is the minor allele with a frequency of 0.45. Genotyping was repeated for several

180 individuals by PCR to verify that the custom probe was working properly (S3 Fig). For
181 comparison, the *HCN2*-NRS was also genotyped in the African Ancestry in Southwest USA
182 (ASW) and British from England and Scotland (GBR) DNA panels from the 1000 genomes
183 project. *HCN2*-NRS was not as common in these two ethnic groups with frequencies of 0.03 and
184 0.15 in the ASW and GBR populations, respectively. Despite being enriched in IAZ, the *HCN2*-
185 NRS allele was not significantly associated with any obesity or type 2 diabetes-related traits which
186 are highly prevalent in this population (data not shown).
187

188 **Structural variation in the *de novo* assemblies**

189 Structural variants (SV) were analyzed directly from the *de novo* assemblies using Assemblytics,
190 which distinguishes between insertions/deletions and contractions/expansions of repeat elements
191 [20]. A total of 12,265 and 12,133 SVs were detected for Sample 1 and Sample 2, respectively,
192 which is similar to an Assemblytics report for a human reference assembly (11,206 SVs) [20] but
193 lower than the number of SVs reported in other studies that used assembly-based or long-read
194 mapping approaches [18, 21]. The lower number of SVs in our study can be attributed to the
195 stringency of our SV detection method. For both samples, the larger SVs (500bp–10,000bp) are
196 predominately composed of tandem expansions (S4 Fig). The distribution graphs also show peaks
197 of SV counts at around 300 bp and 6,000 bp (S4 Fig), a size distribution pattern similar to a
198 previous report [18].
199

200 **Variant calling using the amended hg38-NRS map**

201 Variant calling using our short-read WGS data generated for 387 IAZ individuals and the amended
202 hg38-NRS map identified 11,130,171 variants. Using the new hg38-NRS map identified 161,502

203 gained single nucleotide variants (SNVs) including 695 missense substitutions that were not
204 captured when variant calling was performed using the hg38 reference map (Fig 3). Additionally,
205 180,940 SNVs that were captured using the hg38 map were not detected (lost) with the hg38-NRS
206 map (Fig 3). Most of the gained SNVs (n = 111,976) were low-frequency variants; while the
207 remaining gained SNVs (n = 49,526) were detected in ≥ 5% of the WGS samples. The accuracy
208 of our variant calling with the hg38-NRS map was assessed by sequencing 25 gained SNVs (15
209 reported and 10 not reported in dbSNP). For the 15 dbSNPs, 13 of the gained SNVs were verified
210 and for the 10 non-dbSNPs, 6 were validated. Most of the non-dbSNPs SNVs reside in repetitive
211 regions of the genome which may account for the reduced accuracy.
212

213 **DISCUSSION**

214 In this study, our goal was to enhance the identification of genetic variations that remain largely
215 unexplored within an Indigenous American cohort from Arizona. We focused on identifying NRSs
216 in *de novo* genome assemblies constructed for the two participants from the IAZ cohort. The newly
217 identified NRSs signify novel genomic regions not found in the current GRCh38/hg38 reference
218 map. By incorporating these NRS segments into our WGS variant calling pipeline, we aimed to
219 uncover previously undetected polymorphisms.

220 The *de novo* assemblies were constructed using long-read PacBio HiFi sequencing which produces
221 highly accurate long-read (>10 kb) sequencing data [22]. The sizes for the *de novo* genome
222 assemblies were similar to hg38 and exhibited high contiguity with a mean N50 value of 42.2 Mb.
223 We identified > 10,000 SVs per *de novo* genome assembly which is in line with the expectations
224 for long-read sequencing [23]. This assembly-based approach for SV detection proved particularly
225 advantageous for capturing variants of substantial size [24], and the categorization facilitated by

226 Assemblytics allowed us to differentiate between SVs occurring in repetitive regions, such as
227 tandem expansions and repeat contractions, and those in non-repetitive regions
228 (insertions/deletions). It is worth noting that the largest insertions and deletions (> 500 kb) often
229 resided in regions characterized by high repeat content. We discovered 220 shared deletions (>
230 500 kb) in both *de novo* assemblies with 90 SVs located within genes (data not shown). The
231 application of a high-throughput genotyping approach with custom CNV probes could potentially
232 reveal commonly occurring deletions and uncover potential associations with diseases. However,
233 probe designs for these regions, predominantly repetitive in content, would pose a challenge.
234 The detected NRSs in two assemblies were found to be highly enriched in repeat sequences,
235 especially satellites and simple repeats. This high repeat content was consistent with the previous
236 literature on non-reference genomic parts [21, 25], and rendered the precise placement of NRSs
237 into chromosomes challenging. We identified 1.5 Mb of non-repetitive NRS per assembly and 241
238 kb was anchored to specific chromosomal regions in the primary assembly of hg38. The largest
239 NRS (215 kb) was anchored to chrY. This large NRS is probably a result of chrY being incomplete
240 in the current hg38 map due to its complex repeat structure [26].
241 Several of the NRSs anchored to intronic regions and we focused on a particular NRS in *HCN2*.
242 *HCN2*-NRS was detected in both de novo assemblies and genotyping showed that the *HCN2*-NRS
243 allele is common (MAF = 0.45) in the IAZ population. We also determined that *HCN2*-NRS is
244 present in Caucasians and African Americans but at lower frequencies (MAF = 0.15 and 0.03,
245 respectively).
246 The *HCN2*-NRS matches (100% identity) with a region located downstream of exon 4 that
247 encompasses a putative *cis*-regulatory element suggesting that individuals carrying the *HCN2*-
248 NRS may have additional transcription factor binding sites which may potentially influence gene

249 expression. *HCN2* encodes for a voltage-gated cation channel predominantly expressed in the heart
250 and the brain and plays a crucial role in migraine, inflammatory, and neuropathic pain including
251 diabetic neuropathy [27-29]. HCN2 ion channels initiate neuropathic pain by modulating action
252 potential firing in nociceptor neurons involved in sensing pain intensity [30].
253 Compared to Caucasians, chronic widespread and localized musculoskeletal pain disorders are
254 uncommon among IAZ [31], however, IAZ have high rates of diabetic neuropathy and pain from
255 rheumatoid arthritis [32, 33]. It is possible that the common *HCN2*-NRS allele might modestly
256 contribute to diabetic neuropathy since there are multiple rare intronic variants with nominal
257 associations with diabetic neuropathy reported in the T2D Knowledge Portal
258 (https://t2d.hugeamp.org/). However, the current study has no data on diabetic neuropathy pain to
259 address this hypothesis.
260 Our validation assessment for "gained" variants, namely the subset of genomic variants that were
261 only called using hg38-NRS as the reference, using Sanger sequencing underlines the reliability
262 of our WGS data analysis with the extended reference map. However, the calls arising from
263 repetitive regions provided lower rates of true positives. Further research is needed to understand
264 the functional significance of the gained variants and potential contributions to diseases among
265 IAZ population.
266 The overall findings we presented have expanded our understanding of genetic diversity within
267 Indigenous American populations. The presence of unique genetic elements and variants
268 unrepresented in existing reference maps demonstrates the importance of delving into the
269 genomics of underrepresented populations. By combining long-read sequencing and novel NRS
270 identification methods, we were able to uncover previously elusive genetic variations. This study
271 not only highlights the value of studying isolated populations but also emphasizes the need for

diverse and comprehensive reference maps to accurately capture the complexity of human genetic diversity. Our work contributes to the broader goal of enhancing genomic research's inclusivity and represents a step toward more precise understanding of genetic factors underlying health disparities in underrepresented populations.

METHODS

Long-read sequencing and *de novo* assembly

Two DNA samples isolated from one female and one male individual were sequenced using the PacBio HiFi SMRT sequencing platform at the DNA Sequencing Center at Brigham Young University (Provo, UT). SMRT bell adapted DNA libraries were size selected and ~15 kb fractions were run on 3 SMRT cells (8M trays) for a duration of 30 hours for each sample. Bioinformatic analysis for the construction of the IAZ *de novo* assemblies was done by the DNA Sequencing Center at Brigham Young University. Selected quality reads were assembled using Hifiasm version 0.11 (r302). Continuity of the reads and other summary statistics were calculated using the caln50 package (https://github.com/lh3/calN50).

Detection of non-reference sequences and structural variants in the *de novo* assemblies

All computational analyses were run on the high-performance computing environment NIH HPC Biowulf cluster (http://hpc.nih.gov). Visualization was performed on RStudio using ggplot2 package of R (version 4.3.1).

The *de novo* assemblies were compared to the Genome Reference Consortium Human Build 38 patch release 13 (GRCh38.p13/hg38) using the alignment script of NUCmer from the MUMmer package (version 4.0.0beta2). Each assembly was aligned to GRCh38.p13/hg38 with the

296 parameters --maxmatch -l 150 -c 400. The resulting alignments were filtered to retain only the
297 single best alignment for each contig using the delta-filter -q command. The show-coords tool was
298 then used to extract the coordinates and percent identity of the aligned contigs. To identify the
299 contigs that failed to align to hg38 (< 80% sequence identity), a custom script (available at
300 https://github.com/cigdemkoroglu/NRS/blob/main/unaligned_contigs.R) was used to parse the
301 output of the alignment and extract the unaligned contigs and contigs with low identity. Bedtools
302 version 2.29.2 was employed to generate fasta files containing only the unaligned portions of the
303 assemblies (NRSs). To improve the alignment sensitivity and capture more contigs, the alignment
304 workflow was repeated on the initial output of NRSs with relaxed NUCmer settings (--maxmatch
305 -l 100 -c 200). This allowed for a more permissive alignment approach to increase the number of
306 contigs that could be aligned to the reference. Final NRSs were analyzed for repetitive sequences
307 using RepeatMasker and Assemblytics was used to detect structural variants > 50 bp
308 (http://assemblytics.com/).
309

310 **Anchoring the NRSs to the GRCh38.p13/hg38 primary assembly**

311 For each NRS, 100 bp of flanking sequences either side of the NRSs were aligned to the nucleotide
312 collection database using the blastn. Contigs from the *de novo* assemblies with both flanking sites
313 anchoring to the primary assembly chromosomes of hg38 were selected and appended to hg38 to
314 generate an extended reference genome (hg38-NRS) using perEditor
315 (https://systemsbio.ucsd.edu/perEditor/). NRSs spanning a reference region longer than the NRS
316 itself and those aligning to the same region, indicating repeat expansions, were not incorporated
317 into the hg38-NRS reference genome. In cases where NRSs overlapped between both assemblies,
318 only the region from assembly 1 was included.

319

320 **Variant calling using hg38 and hg38-NRS reference genomes**

321 Whole genomes for 387 IAZ individuals were previously sequenced using Illumina short-read
322 chemistry (30× average coverage). Variant discovery was performed in parallel on whole genome
323 sequencing data from 387 IAZ samples using either hg38 or hg38-NRS as the reference. GATK
324 4.2.6 was used following the best practices workflow, which includes base quality score
325 recalibration, variant calling and joint genotyping by HaplotypeCaller and GenotypeGVCFs, and
326 variant quality score recalibration. Databases for the known variation in the GATK resource
327 bundle were position adjusted based on hg38-NRS using a custom lift-over script (available at
328 https://github.com/cigdemkoroglu/NRS/blob/main/lift_database.R). Monomorphic variants,
329 variants with a call rate <95%, variants with quality scores below the truth sensitivity level 99%
330 threshold, and variants with discordant genotypes between the duplicate pairs were removed from
331 the final vcf files using VCFtools.

332

333 **Identification of gained single nucleotide variants (SNVs) in the hg38-NRS reference genome**

334 To compare variant calling between hg38 and hg38-NRS reference genomes, ANNOVAR was
335 first used to annotate the variants identified with hg38. Next, to annotate the variants identified
336 with hg38-NRS and to ensure compatibility between the two reference maps, the hg38-NRS
337 variant dataset was lifted-over using custom scripts (https://github.com/cigdemkoroglu/NRS).
338 Lastly, to identify lost and gained SNVs, the hg38 and hg38-NRS annotated datasets were
339 compared using the LostGained tool (https://github.com/ cigdemkoroglu/NRS/blob/main
340 /LostGained.R). Among the gained variants, 15 missense variants that are reported in dbSNP but
341 were not detected by our in-house genotyping studies using the Affymetrix SNP Array 6.0 or our

342 whole-genome and whole-exome sequencing studies along with 10 randomly selected novel SNVs
343 were verified by sequencing.
344

345 **Genotyping of the *HCN2*-NRS**

346 Genotyping of the *HCN2*-NRS in the Indigenous Americans from Arizona (IAZ) was performed
347 using DNA isolated from 3,410 individuals who participated in a community-based longitudinal
348 study examining type 2 diabetes-related traits conducted by the National Institute of Diabetes and
349 Digestive and Kidney Diseases (NIDDK) in Phoenix, Arizona between the years 1965 and 2007
350 [34]. All participants in the study were self-reported full-heritage Indigenous American (all eight
351 great grandparents identified as IAZ). The *HCN2*-NRS was also genotyped in the African Ancestry
352 in Southwest USA (ASW) and British from England and Scotland (GBR) DNA panels from the
353 1000 genomes project. The ASW and GBR DNA samples were obtained from the NHGRI Sample
354 Repository for Human Genetic Research at the Coriell Institute for Medical Research: Repository
355 IDs MGP00015 and MGP00003, respectively. Genotyping of the *HCN2*-NRS was done using
356 custom designed TaqMan probes that detected the presence of either the reference sequence (RS)
357 or NRS. (Thermo Fisher Scientific, Waltham, MA). Statistical analyses were performed using the
358 software of the SAS Institute (Cary, NC, USA) as previously described [35].
359

360 **Acknowledgments**

361 We thank Chris Wiedrich for his help in genotype validation, Sayuko Kobes for running
362 association tests, and Paolo Piaggi for providing statistical consultation. This work was supported
363 by the Intramural Research Program of the NIDDK, NIH. We utilized the computational resources
364 of the NIH HPC Biowulf cluster (http://hpc.nih.gov).
365

366 **Author contributions:**

367 Conceptualization: Cigdem Koroglu, Clifton Bogardus

368 Study design & data analysis: Cigdem Koroglu

369 Consultation regarding data analysis: Peng Chen

370 Supervision: Leslie J. Baier

371 Software: Serdar Altok, Peng Chen, Cigdem Koroglu

372 Computational troubleshooting: Cigdem Koroglu, Serdar Altok

373 Genotyping: Michael Traurig, Cigdem Koroglu

374 Visualization: Cigdem Koroglu, Michael Traurig

375 Writing -original draft: Cigdem Koroglu

376 Writing -review & editing: Leslie J. Baier, Cigdem Koroglu, Michael Traurig, Peng Chen, Clifton

377 Bogardus, Serdar Altok

378

379 **Competing interests:** The authors declare no competing interests.

380

381 **References**

382 1. Gurdasani D, Barroso I, Zeggini E, Sandhu MS. Genomics of disease risk in globally

383 diverse populations. Nat Rev Genet. 2019; 20(9): 520-535.

384 2. Manrai AK, Funke BH, Rehm HL, Olesen MS, Maron BA, Szolovits P, et al. Genetic

385 Misdiagnoses and the Potential for Health Disparities. N Engl J Med. 2016; 375(7): 655-

386 665.

387 3. Popejoy AB, Fullerton SM. Genomics is failing on diversity. Nature. 2016; 538(7624):

388 161-164.

389 4. All of Us Research Program Investigators; Denny JC, Rutter JL, Goldstein DB, Philippakis
390 A, Smoller JW, et al. The "All of Us" Research Program. N Engl J Med. 2019; 381(7):
391 668-676.
392 5. GenomeAsia100K Consortium. The GenomeAsia 100K Project enables genetic
393 discoveries across Asia. Nature. 2019; 576(7785): 106-111.
394 6. Mulder N, Abimiku A, Adebamowo SN, de Vries J, Matimba A, Olowoyo P, et al.
395 H3Africa: current perspectives. Pharmgenomics Pers Med. 2018; 11: 59-66.
396 7. Chheda H, Palta P, Pirinen M, McCarthy S, Walter K, Koskinen S, et al. Whole-genome
397 view of the consequences of a population bottleneck using 2926 genome sequences from
398 Finland and United Kingdom. Eur J Hum Genet. 2017; 25(4): 477-484.
399 8. Beyter D, Ingimundardottir H, Oddsson A, Eggertsson HP, Bjornsson E, Jonsson H, et al.
400 Long-read sequencing of 3,622 Icelanders provides insight into the role of structural
401 variants in human diseases and other traits. Nat Genet. 2021; 53(6): 779-786.
402 9. Wu Z, Jiang Z, Li T, Xie C, Zhao L, Yang J, et al. Structural variants in the Chinese
403 population and their impact on phenotypes, diseases and population adaptation. Nat
404 Commun. 2021; 12(1): 6501.
405 10. Schneider VA, Graves-Lindsay T, Howe K, Bouk N, Chen HC, Kitts PA, et al. Evaluation
406 of GRCh38 and de novo haploid genome assemblies demonstrates the enduring quality of
407 the reference assembly. Genome Res. 2017; 27(5): 849-864.
408 11. Chaisson MJ, Huddleston J, Dennis MY, Sudmant PH, Malig M, Hormozdiari F, et al.
409 Resolving the complexity of the human genome using single-molecule sequencing. Nature.
410 2015; 517(7536): 608-611.

411 12. Logsdon GA, Vollger MR, Eichler EE. Long-read human genome sequencing and its
412 applications. Nat Rev Genet. 2020; 21(10): 597-614.
413 13. Marx V. Method of the year: long-read sequencing. Nat Methods. 2023; 20(1): 6-11.
414 14. De Coster W, Weissensteiner MH, Sedlazeck FJ. Towards population-scale long-read
415 sequencing. Nat Rev Genet. 2021; 22(9): 572-587.
416 15. Liao WW, Asri M, Ebler J, Doerr D, Haukness M, Hickey G, et al. A draft human
417 pangenome reference. Nature. 2023; 617(7960): 312-324.
418 16. Redd AJ, Chamberlain VF, Kearney VF, Stover D, Karafet T, Calderon K, et al. Genetic
419 structure among 38 populations from the United States based on 11 U.S. core Y
420 chromosome STRs. J Forensic Sci. 2006; 51(3): 580-585.
421 17. Kim HI, Ye B, Gosalia N; Regeneron Genetics Center; Köroğlu Ç, Hanson RL, et al.
422 Characterization of Exome Variants and Their Metabolic Impact in 6,716 American
423 Indians from the Southwest US. Am J Hum Genet. 2020; 107(2): 251-264.
424 18. Ameur A, Che H, Martin M, Bunikis I, Dahlberg J, Höijer I, et al. De Novo Assembly of
425 Two Swedish Genomes Reveals Missing Segments from the Human GRCh38 Reference
426 and Improves Variant Calling of Population-Scale Sequencing Data. Genes (Basel). 2018;
427 9(10): 486.
428 19. Gao Y, Yang X, Chen H, Tan X, Yang Z, Deng L, et al. A pangenome reference of 36
429 Chinese populations. Nature. 2023; 619(7968): 112-121.
430 20. Nattestad M, Schatz MC. Assemblytics: a web analytics tool for the detection of variants
431 from an assembly. Bioinformatics. 2016; 32(19): 3021-3023.

432 21. bert P, Audano PA, Zhu Q, Rodriguez-Martin B, Porubsky D, Bonder MJ, et al. Haplotype-
433 resolved diverse human genomes and integrated analysis of structural variation. Science.
434 2021; 372(6537): eabf7117.
435 22. Hon T, Mars K, Young G, Tsai YC, Karalius JW, Landolin JM, et al. Highly accurate long-
436 read HiFi sequencing data for five complex genomes. Sci Data. 2020; 7(1): 399.
437 23. Ho SS, Urban AE, Mills RE. Structural variation in the sequencing era. Nat Rev Genet.
438 2020; 21(3): 171-189.
439 24. Mahmoud M, Gobet N, Cruz-Dávalos DI, Mounier N, Dessimoz C, Sedlazeck FJ.
440 Structural variant calling: the long and the short of it. Genome Biol. 2019; 20(1): 246.
441 25. Li R, Tian X, Yang P, Fan Y, Li M, Zheng H, et al. Recovery of non-reference sequences
442 missing from the human reference genome. BMC Genomics. 2019; 20(1): 746.
443 26. Skaletsky H, Kuroda-Kawaguchi T, Minx PJ, Cordum HS, Hillier L, Brown LG, et al. The
444 male-specific region of the human Y chromosome is a mosaic of discrete sequence classes.
445 Nature. 2003; 423(6942): 825-837.
446 27. Young GT, Emery EC, Mooney ER, Tsantoulas C, McNaughton PA. Inflammatory and
447 neuropathic pain are rapidly suppressed by peripheral block of hyperpolarisation-activated
448 cyclic nucleotide-gated ion channels. Pain. 2014; 155(9): 1708-1719.
449 28. Tsantoulas C, Ng A, Pinto L, Andreou AP, McNaughton PA. HCN2 Ion Channels Drive
450 Pain in Rodent Models of Migraine. J Neurosci. 2022; 42(40): 7513-7529.
451 29. Tsantoulas C, Laínez S, Wong S, Mehta I, Vilar B, McNaughton PA. Hyperpolarization-
452 activated cyclic nucleotide-gated 2 (HCN2) ion channels drive pain in mouse models of
453 diabetic neuropathy. Sci Transl Med. 2017; 9(409): eaam6072.

454 30. Emery EC, Young GT, Berrocoso EM, Chen L, McNaughton PA. HCN2 ion channels play
455 a central role in inflammatory and neuropathic pain. Science. 2011; 333(6048): 1462-1466.
456 31. Jacobsson LT, Nagi DK, Pillemer SR, Knowler WC, Hanson RL, Pettitt DJ, et al. Low
457 prevalences of chronic widespread pain and shoulder disorders among the Pima Indians. J
458 Rheumatol. 1996; 23(5): 907-909.
459 32. Jaiswal M, Fufaa GD, Martin CL, Pop-Busui R, Nelson RG, Feldman EL. Burden of
460 Diabetic Peripheral Neuropathy in Pima Indians With Type 2 Diabetes. Diabetes Care.
461 2016; 39(4): e63-64.
462 33. Del Puente A, Knowler WC, Pettitt DJ, Bennett PH. High incidence and prevalence of
463 rheumatoid arthritis in Pima Indians. Am J Epidemiol. 1989; 129(6): 1170-1178.
464 34. Knowler WC, Bennett PH, Hamman RF, Miller M. Diabetes incidence and prevalence in
465 Pima Indians: a 19-fold greater incidence than in Rochester, Minnesota. Am J Epidemiol.
466 1978; 108(6): 497-505.
467 35. Day SE, Traurig M, Kumar P, Piaggi P, Koroglu C, Kobes S, et al. Functional variants in
468 cytochrome b5 type A (CYB5A) are enriched in Southwest American Indian individuals
469 and associate with obesity. Obesity (Silver Spring). 2022; 30(2): 546-552.

470

471 **Figure legends**

472 **Fig 1**

473 Histograms depicting the length distribution of NRSs identified in the indigenous Sample 1 (panels
474 A to C) and Sample 2 (panels D to F). Dashed lines represent the median values for each histogram.
475 **A**. Small NRSs ranging from 100 bp and 10 kb, with a median length of 776 bp. **B**. NRSs sized
476 between 10 kb and 100 kb, with a median size of 20.5 kb. **C**. NRSs longer than 100 kb are shown,

477 with a median size of 192 kb. Except for two outliers indicated by arrows, all NRSs in this group
478 are shorter than 500 kb. The arrows in this panel highlight a 637 kb NRS and a 1.88 Mb NRS, both
479 of which consist of simple repeats and microsatellites, and do not align to any hg38 contigs with
480 high sequence identity. **D**. Small NRSs with varying lengths between 100 bp and 10 kb and with
481 a median length of 617 bp. **E**. NRSs sized between 10 kb and 100 kb. The median size is 22.7 kb.
482 **F**. NRSs longer than 100 kb, with a median size of 187.8 kb. There is a single NRS, marked with
483 an arrow, exceeding 500 kb in length. This 1.47 Mb NRS comprises solely of simple repeats and
484 microsatellites, and does not anchor to any hg38 contigs.

485 **Fig 2**

486 *HCN2*-NRS and chr19-RS side by side alignment. Source: UCSC Genome Browser
487 (GRCh38/hg38).

488 **Fig 3**

489 Number of SNVs gained (light gray) and lost (dark gray) per chromosome for the cohort of 387
490 short-read WGS samples when analyzed with the hg38-NRS map compared to hg38 map.

Figure 1

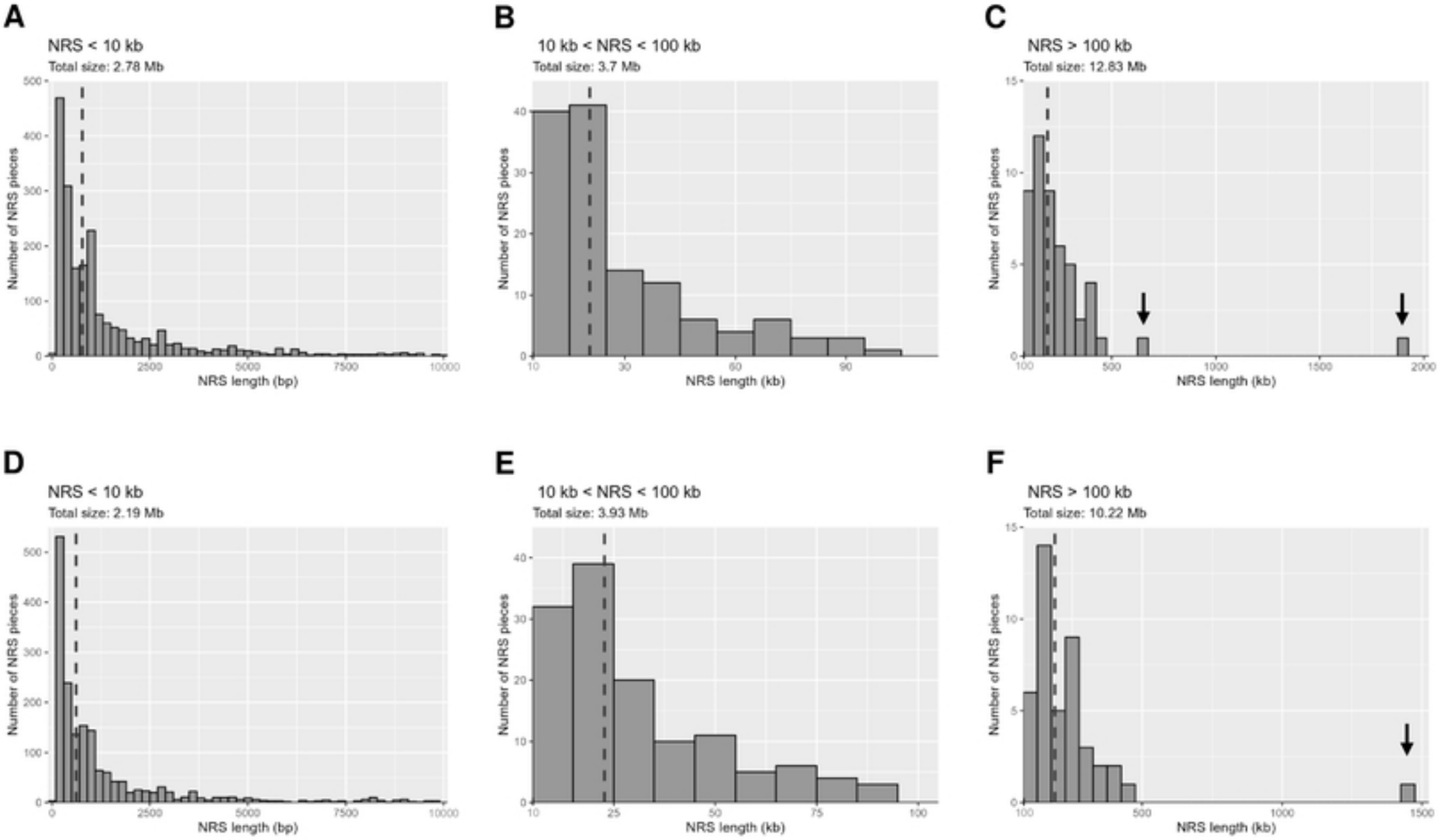

Figure

Figure 2

Size	Identity	Chromosome	Strand	Start	End
187 bp	100%	19	+	608436	608622

```
HCN2-NRS 000001 caagtggcgcgctcagggcagagaccgcgtgatggggagcaggggaccct 000050
         >>>>>> |||||||||||||||||||||||||||||||||||||||||||||||| >>>>>>
 Chr19-RS 608436 caagtggcgcgctcagggcagagaccgcgtgatggggagcaggggaccct 608485

HCN2-NRS 000051 gggggtctgtggctgtgattaggaggagaaacggccggtggtgagaggtt 000100
         >>>>>> |||||||||||||||||||||||||||||||||||||||||||||||| >>>>>>
 Chr19-RS 608486 gggggtctgtggctgtgattaggaggagaaacggccggtggtgagaggtt 608535

HCN2-NRS 000101 ctctgaccctgtgacagggagggaggtccagagcctggagatggacgtgg 000150
         >>>>>> |||||||||||||||||||||||||||||||||||||||||||||||| >>>>>>
 Chr19-RS 608536 ctctgaccctgtgacagggagggaggtccagagcctggagatggacgtgg 608585

HCN2-NRS 000151 ggcgggggctggggaggggatgcaggctgggcaggaa 000187
         >>>>>> |||||||||||||||||||||||||||||||||||| >>>>>>
 Chr19-RS 608586 ggcgggggctggggaggggatgcaggctgggcaggaa 608622
```

Figure

Figure 3

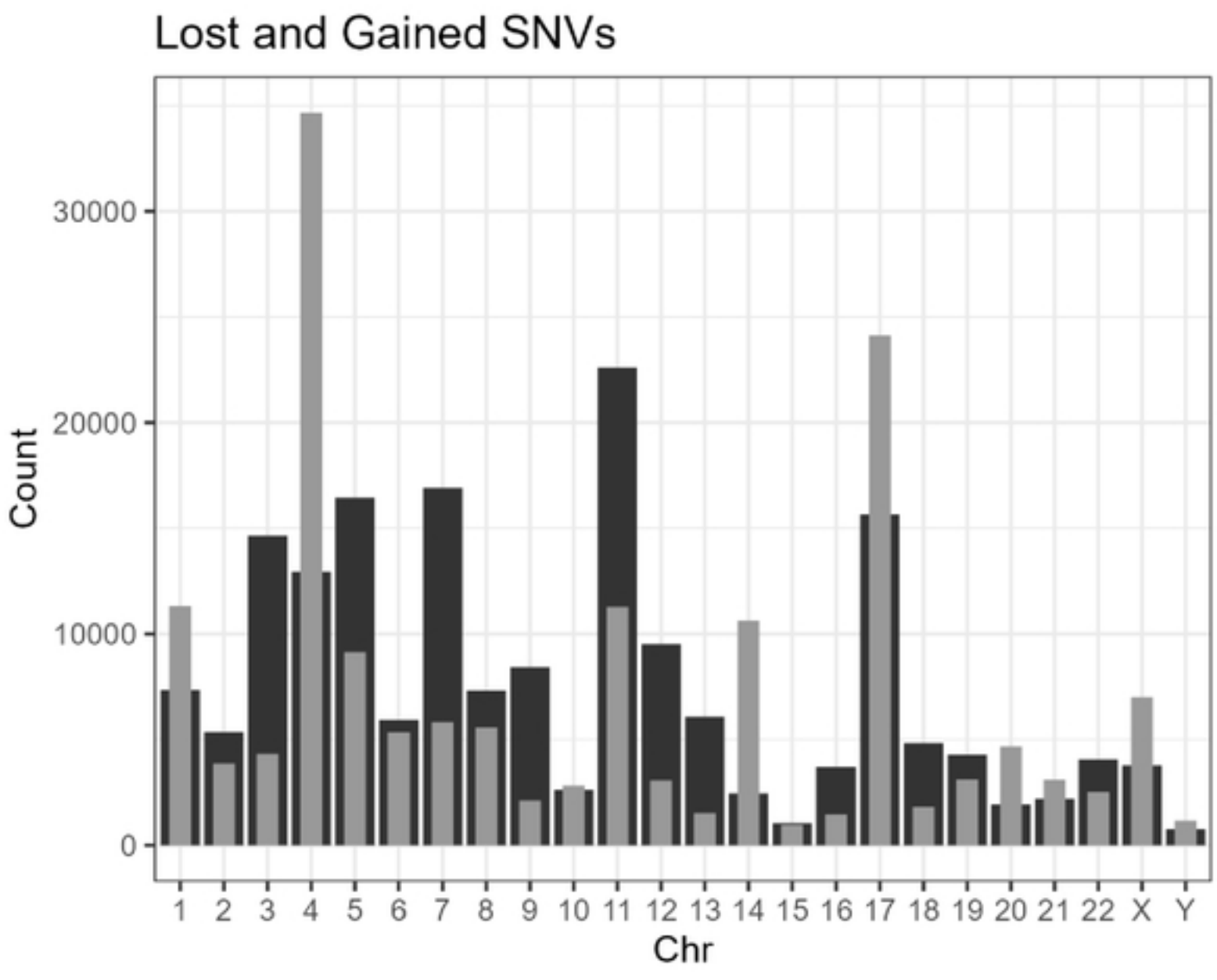

Figure